Proc. Natl. Acad. Sci. USA
Vol. 84, pp. 5735–5739, August 1987
Biophysics

Molecular mechanical simulations on double intercalation of 9-amino acridine into d(CGCGCGC)·d(GCGCGCG): Analysis of the physical basis for the neighbor-exclusion principle

(molecular dynamics/counterion/conformation/normal mode/entropy)

SHASHIDHAR N. RAO AND PETER A. KOLLMAN*

Department of Pharmaceutical Chemistry, School of Pharmacy, University of California, San Francisco, CA 94143

Communicated by I. Tinoco, Jr., February 9, 1987 (received for review December 22, 1986)

ABSTRACT **The neighbor-exclusion principle is one of the most general and interesting rules describing intercalative DNA binding by small molecules. It suggests that such binding can only occur at every other base-pair site, reflecting a very large negative cooperativity in the binding process. We have carried out molecular mechanics and molecular dynamics simulations to study intercalation complexes between 9-amino acridine and the base-paired heptanucleotide d(CGCGCGC)·d(GCGCGCG), in which the neighbor-exclusion principle was both obeyed and violated. Our studies find no stereochemical preference that favors the neighbor-exclusion-obeying structures over the neighbor-exclusion-violating structures. Alternative explanations for the existence of the neighbor-exclusion principle are vibrational entropy effects that we calculate to favor the more flexible neighbor-exclusion models over the more rigid neighbor-exclusion-violating models and polyelectrolyte (counterion release) effects.**

The neighbor-exclusion principle proposed by Crothers (1) is one of the most general rules for intercalative binding of planar drugs to DNA. According to this principle, every second (next-neighbor) intercalation site along the length of the DNA double helix remains unoccupied. Experimental evidence for this principle has been found in fiber diffraction studies on nucleic acid fibers bound to metallointercalative agents (2, 3), in single-crystal studies (4–8) on complexes between dinucleoside monophosphates complexed with intercalating drugs, and solution studies on binding of ethidium ion to oligonucleotides of ribose and deoxyribose sugars (9). Based on earlier crystallographic studies (4–6) that suggested mixed sugar puckering at the intercalation site, a stereochemical basis for the neighbor-exclusion principle was proposed. However, this mixed sugar puckering scheme has not been shown to be essential for creating intercalating sites in double-helical DNA through several crystal structure and model building studies (7–11).

The first evidence suggesting violation of the neighbor-exclusion model was obtained from viscometric studies (12–14) on interactions between bi- and triderivatives of acridine and DNA, where it was suggested that a single base pair was sandwiched between two acridines. ^{1}H NMR studies on the binding of a series of bis(acridine) compounds to $d(AT)_5 \cdot d(AT)_5$, in which the two acridine rings were linked through linker chains of various lengths, found no evidence of violation of the neighbor-exclusion principle (15, 16). However, it was also noted that these studies have not ruled out violation of the neighbor-exclusion principle under different salt conditions and temperatures or a different nucleotide sequence (15). It has been postulated (17) that the anticooperativity of ethidium binding to DNA could be explained without reference to the neighbor-exclusion rule and is solely due to polyelectrolyte effects.

Why do some simple monofunctional intercalators such as 9-amino acridine not intercalate at neighboring sites and violate the neighbor-exclusion principle? In this paper, we present theoretical investigations into the energetic basis for the neighbor-exclusion principle. Crystallographic data on complexes between oligonucleotides containing three or more base pairs and only intercalating drugs daunomycin (18) and triostin (19) are available. This limited data and the lack of sufficient experimental data on violation of neighbor-exclusion models make the theoretical investigations a challenging task. Model-building and energy-minimization studies on deoxytetranucleotides have been used to investigate the possibilities of creating intercalation sites obeying and violating the nearest-neighbor rule, in the framework of helical structures (20). Sawaryn *et al.* (21) have reported energy calculations on neighbor-exclusion models using an idealized dinucleoside monophosphate system to "create" structures violating this principle, but those calculations are very limited in scope. In the present investigations, we have considered the double intercalation of 9-amino acridine into the base-paired heptadeoxyribonucleotide d(CGCGCGC)·d(GCGCGCG) and have model built both neighbor-exclusion-obeying and -violating structures. These structures will be called Oby and Vio, respectively. We find, using molecular mechanics and molecular dynamics simulations, that it is possible to build energetically reasonable structures with and without the neighbor-exclusion principle being violated by the intercalating molecules. Entropy effects could be a critical factor in the neighbor-exclusion principle.

METHODS

Intercalation geometries were created using the computer graphics program CHEM (22) on the E and S PS2 at the computer graphics laboratory of the University of California at San Francisco in the following way. The oligonucleotide was "cut" on the two chains at the phosphates in the intercalation site. Then, the two double-stranded segments were separated along the helix axis till the distance between the base pairs on either side of the cut was ≈7 Å. The two segments were then rotated relative to one another about the helix axis to achieve maximum overlap between these two base pairs. The planar acridine was then intercalated between the two base pairs, and the backbone dihedrals (except the sugar geometry) in intercalation sites were altered to minimize the distance between the bonded atoms. These model-built structures were then subjected to energy minimizations using the program AMBER(UCSF) (23–25).

The publication costs of this article were defrayed in part by page charge payment. This article must therefore be hereby marked "*advertisement*" in accordance with 18 U.S.C. §1734 solely to indicate this fact.

Abbreviations: Oby and Vio, structures that obey or violate, respectively, the neighbor-exclusion principle.

The molecular mechanical energies were evaluated by using equation 1 in ref. 23 with the force field parameters presented by Weiner *et al.* (26), and the structures were energy refined until an rms gradient of 0.1 kcal/mol·Å (1 cal = 4.184 J) was achieved. In all the calculations a distance-dependent dielectric constant was used (26). The charges on 9-amino-acridine (Fig. 1) were determined using the quantum chemically derived electrostatic potentials (27) with a STO-3G basis set and can be obtained from the authors. The equilibrium values for C—C, N—C, and N—H bond lengths in 9-amino acridine were taken as 1.378, 1.40, and 1.01 Å, respectively, with the corresponding force constants being 480, 460, and 434 kcal/mol, respectively. All the bond angles had equilibrium values of 120° with a force constant of 80 kcal/mol. The dihedral force constants were chosen to be the same for analogous dihedral angles in proteins and nucleic acids (26).

The energy-minimized structures have been labeled as Oby1 and Vio1, corresponding to the two classes of model-built complexes mentioned above. Constrained energy minimizations were also carried out (as detailed in a later section) in which a few heptamer backbone torsions were constrained to take up specific values, using a dihedral force constant of 100 kcal/mol. The structures thus obtained were further refined, after removing the constraints, to compare their relative stabilities to the structures obtained after energy minimizations with no constraints. In addition, we have also energy minimized the heptanucleotide in the B form without the intercalators.

In addition to molecular mechanical simulations, molecular dynamical simulations were also carried out on the energy-refined structures Oby and Vio, with a view to explore the conformational space around the minima. This was done using the molecular dynamics module in the program AMBER(UCSF) on the VAX11/780 with an FPS-264 attachment (25). These simulations were carried out at 300 K for a 50-ps time period in "hydrated" sodium counterions (28) that were placed along the bisector of the pendant oxygens in the phosphate groups at distance of 5 Å.

Initially, unconstrained dynamics were carried out in which the entire system, consisting of the heptamer, the two acridines, and counterions, was allowed to move. This led to structures in which the acridines were not fully intercalated between the base pairs but were hydrogen bonded to phosphates and bases in the vicinity of intercalation site through the N10—H10 and 9-amino groups. To avoid such large distortions of the structures, which are due to our primitive treatment of electrostatic effects, we constrained the central base pairs (four in Vio and five in Oby) in and around the intercalation sites to their coordinates obtained after energy refinement of initial model-built structures (Oby1 and Vio1). The molecular dynamics simulations were then carried out with freedom of movement in cartesian space being allowed to the rest of the system, namely, the end base pairs, both oligonucleotide backbones, the acridines, and the counterions. Structures obtained at the end of every 5 ps in such a simulation were then subjected to energy minimization in the presence of counterions until the above stated gradient criterion was achieved. All of these structures are numbered as, for example, Oby2 and Vio2.

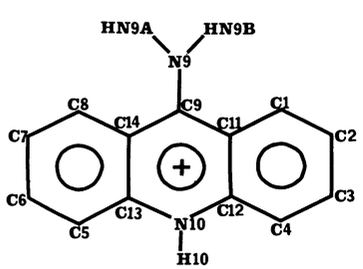

FIG. 1. Schematic representation of 9-amino acridine (in the united atom representation) protonated at N10 used in the double-intercalation complexes with d(CGCGCGC)·d(GCGCGCG).

We have also carried out normal mode analysis and thermochemistry calculations on the energy-minimized structures obtained in the molecular-mechanics simulations and have computed the entropy of the two structures using normal mode analysis (25). The energies of the molecular mechanically simulated structures were further refined to very low gradients (10^{-5} kcal/mol·Å), and the resultant structures were entered into the normal mode program to determine the normal modes and thermochemical parameters.

In the two structures that were model built and energy refined, the starting structure of the oligonucleotide was B-DNA (29). The nucleotides in the DNA fragment are referred to by the serial number of the base and the base name with the numbering being continuous into the second strand. Thus, Cyt-3 and Gua-12 are paired in the Watson–Crick configuration. In Vio, one of the acridines was intercalated between the base pairs Cyt-3·Gua-12 and Gua-4·Cyt-11, while the other acridine was intercalated between the base pairs Cyt-5·Gua-10 and Gua-4·Cyt-11. In Oby, the first acridine was intercalated between Gua-2·Cyt-13 and Cyt-3·Gua-12 base pairs, while the second one was intercalated between Cyt-5·Gua-10 and Gua-4·Cyt-11. The two acridines will be referred to as acridine 1 and acridine 2, where the former lies at the 5′ side of strand 1 (containing Cyt-1) in either structure.

RESULTS

Conformations of the Heptanucleotides in Oby and Vio. As expected, the alterations in the conformations of the oligonucleotides in the two double-intercalation complexes from values typical of B-DNA are predominantly confined to the regions of intercalation. The conformations of the oligonucleotide backbone and bases in the regions of intercalation (covering Cyt-3, Gua-4, Cyt-5, and Gua-6 and their complementary base-paired nucleotides in Oby1 and Cyt-3, Gua-4, and Cyt-5 and their complementary base-paired nucleotides in Vio1) are listed in Table 1. Also listed in this table are the backbone and glycosidic conformations in the crystal structures of 9-amino acridine complexed with 5-iodo-CpG (31) and triostin–d(CGTACG) (19). The conformation that differs most significantly between the crystals and theoretical models is the sugar geometry at the 5′ end of the intercalation site.

Table 1. Conformational parameters

	Oby1				Vio1				9AA–CpG		Trio	
Torsion	S1		S2		S1		S2		S1	S2	I1	I2
ζ(5′)	160	124	147	164	148	158	144	158	72	85	138	88
α	180	182	186	179	180	190	186	191	236	216	177	197
β	275	264	262	224	311	270	185	274	311	296	180	307
γ	286	288	278	273	187	177	188	170	280	300	329	206
δ	173	175	178	166	190	173	196	171	220	229	159	143
ε	58	61	58	55	182	180	176	179	67	38	6	55
ζ(3′)	132	147	150	88	158	147	158	143	110	130	133	84
χ(5′)	75	61	68	107	67	68	87	72	17	38	100	94
χ(3′)	72	63	76	32	68	70	72	66	119	109	113	82

Conformational parameters (in degrees) in the intercalation sites of Oby1, Vio1, and crystal structures of intercalation complexes 5-iodo-CpG–9-amino acridine (9AA–CpG) (29) and triostin–d(CGTACG) (Trio) (18). S1 and S2 refer to the two strands of the oligonucleotide duplex, while I1 and I2 refer to the two intercalation sites in Trio (only the backbone and glycosidic conformations of one of the two strands were reported in ref. 18). The nomenclature for the representation of torsion angles in the backbone of nucleic acids is that adopted by Seeman *et al.* (30).

In the latter, they are predominantly in the C2′ *endo* region, while in the crystals, they are predominantly C3′ *endo*.

Only two kinds of conformations not usually seen in the crystal structures either of the complexes between simple intercalators and deoxyoligonucleotides or of deoxyoligonucleotides alone have been observed in the energy-refined models obeying and violating the neighbor-exclusion principle. They are the (*trans,trans*) phosphodiester conformations (β,γ) as at the 3′ end of Cyt-3 in Vio1 and Vio1′ and a *gauche*$^+$ conformation about C5′—O5′ (δ) as at the 5′ end of Cyt-3 in Oby complexes. The unusual phosphodiester conformation leads to a slightly more stretched helix in the case of models violating the neighbor-exclusion principle. Though this conformation has never been observed in DNA structures, it is not uncommon in the structures of tRNA (32). The unusual conformation about C5′—O5′ has been shown to be of reasonable energy in conformational energy calculations on dinucleoside monophosphates (33). Figs. 2 and 3 show stereo views of the energy-refined complexes Oby1 and Vio1.

The conformational properties of Oby and Vio structures are reflected in the overall helical properties of the heptamer duplex in them. For example, the helix in Vio1 is longer than in Oby1 by ≈1.5 Å, due to the stretched (*trans,trans*) phosphodiester conformations in Vio1. The twist and tilts of most of the base pairs in these two structures are similar to those in the B-DNA (Figs. 2 and 3). The only exception is in Vio1, where the twist of the base pairs involving Gua-4 is less by 10° than in the energy-minimized heptamer alone. The overall helix is kinked slightly more in Vio1 (by ≈7°) than in Oby1. In Oby1, the helix is hardly unwound at the first intercalation site involving Cyt-3 and Gua-4, whereas the extent of unwinding is ≈20° at the other site. In Vio1, however, the unwinding is smaller (≈13°) at the first intercalation site. The overall unwinding of the helixes in Oby1 and Vio1 are, respectively, 20° and 10°. These values lie in the range (−3° to 26°) obtained from x-ray crystal studies on complexes between dinucleoside monophosphates and intercalators (see chapter 16 in ref. 34). However, the total unwinding angle for Oby1 is higher than that in daunomycin–d(CGTACG) (16°) (18) and circular DNA (11°) (35) but is lower than in the triostin–d(CGTACG) (19) complex (27°). These differences could be due to several structural factors induced by the intercalation of the more complex drugs in the experimental studies such as Hoogsteen base-pair formation (19).

Energetics. Table 2 lists the molecular mechanical energies of the Vio and Oby structures. The energy components in these two classes of structures obtained by molecular mechanical simulations alone are Oby1, Vio1, and Vio1′. The energy components of the structures obtained with the combination of molecular dynamics and molecular mechanics simulations are Oby2–Oby10 and Vio2–Vio10. To obtain a detailed understanding of the relative energies of the two classes of structures, we have calculated the helix energy (the energy of the heptanucleotide part of the intercalation complexes), helix destabilization energy (difference between the helix energy and the energy of the minimized heptanucleotide in the absence of the acridines), and energy of the central pentamer, drug energy, and drug–helix interaction energies. In the cases of structures simulated with the counterions, the DNA–counterion interaction energies are also listed.

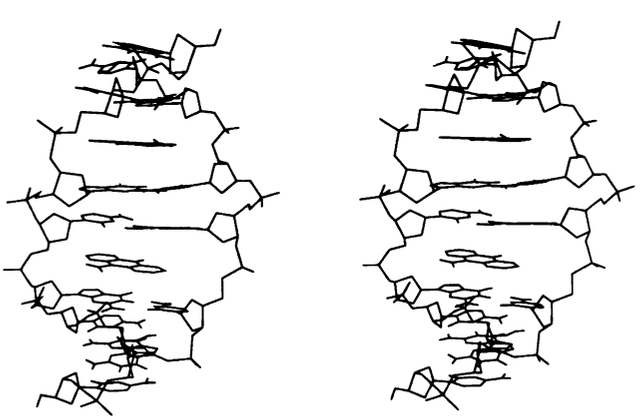

FIG. 2. Stereo view of the double-intercalation complex between d(CGCGCGC)·d(GCGCGCG) and 9-amino acridine, in which the neighbor-exclusion principle is obeyed (structure Oby1).

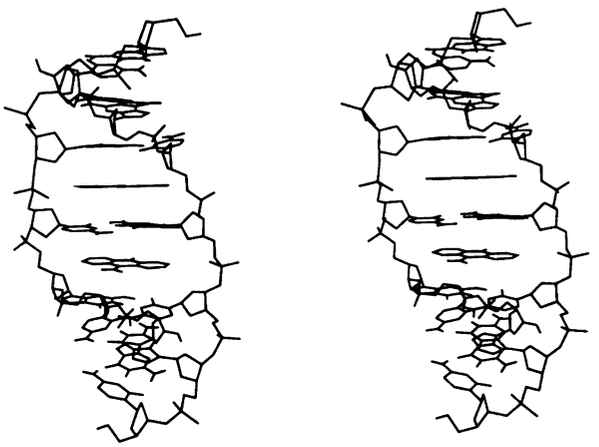

FIG. 3. Stereo view of the double-intercalation complex between d(CGCGCGC)·d(GCGCGCG) and 9-amino acridine, in which the neighbor-exclusion principle is violated (structure Vio1).

The complex Vio1′ is lower in energy than Vio1 by about 6 kcal/mol. This difference is attributed to the more stretched phosphodiester conformation at the 3′ end of Cyt-3 in the former. This helps to reduce the electrostatic repulsion between the phosphate groups around the site of intercalation. In the light of this, the helix destabilization is smaller in Vio1′ than in Vio1, but the drug–helix and drug–drug interactions are not significantly different.

We find that the total energies of the molecular mechanically simulated and energy-refined structures Oby1 and Vio1 are similar. The drug–helix interaction energies are favored in Oby1 by about 5 kcal/mol; however, this is compensated by larger helix destabilization in this structure by a similar amount. The interaction energies between the two intercalators in these two structures differ by <0.5 kcal/mol. Thus, with a distance-dependent dielectric constant, drug–drug interactions in Oby are not much less than in Vio.

In the molecular dynamically simulated structures, the drug–helix and helix destabilization energies vary over a wide range of values that overlap between the two classes of structures. The marginally higher stability of helixes in the Vio structures can be attributed to the more favored electrostatic interactions in them relative to Oby structures. This could be due to the slightly more stretched nature of the oligonucleotide backbone in the intercalation region that leads to a reduction in the repulsion between charged phosphate groups. The presence of counterions does not influence this difference. An analysis of the drug–helix interaction energies reveals that in both classes of complexes, the nonbonded interactions are similar, whereas the electrostatic term is less favorable in Oby than in Vio.

In view of the simple representation of the counterion atmosphere and lack of explicit representation of solvent effects, it is likely that the effects of electrostatic interactions are overemphasized, leading to the slightly greater apparent stability of Vio over Oby complexes. Given such uncertain-

Table 2. The energies of the complexes between two acridines intercalated in d(CGCGCGC)·d(GCGCGCG)

Complex	E_{HDC}	E_{HD}	E_{helix}	E_{destab}	$E_{c\text{-}5}$	$E_{H\text{-}D1}$	$E_{H\text{-}D2}$	$E_{H\text{-}D}$	$E_{H\text{-}Cl}$	$E_{D1\text{-}D2}$	S	N1	N2	N3
Oby1		−750.3	−564.7	56.1	−407.6	−71.0	−74.9	−145.9		1.38	1331	2.3	2.8	3.9
Vio1		−750.6	−569.6	51.2	−413.8	−71.4	−69.4	−140.8		1.73	1323	2.8	3.7	5.0
Vio1′		−756.9	−574.3	46.5	−418.0	−70.9	−71.9	−142.8		1.78	1318	3.0	4.4	5.0
Oby2	−1394.8	−723.3	−538.4	82.4	−389.8	−63.4	−63.9	−127.3	−808.3	1.42				
Oby3	−1397.3	−726.9	−539.1	81.7	−390.6	−62.7	−67.8	−130.5	−808.5	1.46				
Oby4	−1401.0	−727.9	−537.6	83.2	−388.1	−63.0	−69.6	−132.6	−817.7	1.44				
Oby5	−1402.8	−721.5	−537.1	83.7	−387.7	−63.1	−63.7	−126.8	−821.1	1.49				
Oby6	−1410.8	−712.2	−529.5	91.3	−379.6	−62.6	−62.8	−125.4	−840.3	1.52				
Oby7	−1404.8	−716.9	−535.7	85.1	−387.0	−60.0	−64.9	−124.9	−834.5	1.46				
Oby8	−1399.8	−713.7	−538.1	82.7	−390.1	−59.1	−59.5	−118.6	−828.5	1.42				
Oby9	−1405.1	−718.2	−538.4	82.4	−390.9	−60.0	−62.4	−122.4	−829.0	1.41				
Oby10	−1414.1	−713.2	−534.0	86.8	−386.7	−61.3	−60.6	−121.9	−843.0	1.47				
Vio2	−1379.0	−719.5	−540.6	80.2	−397.4	−64.1	−60.6	−124.7	−789.7	1.63				
Vio3	−1379.7	−729.0	−544.6	76.2	−398.7	−68.8	−61.4	−130.2	−783.2	1.72				
Vio4	−1384.0	−725.8	−541.8	79.0	−398.8	−68.7	−60.7	−129.4	−789.5	1.70				
Vio5	−1378.9	−729.1	−543.4	77.4	−397.5	−69.1	−62.4	−131.5	−781.1	1.61				
Vio6	−1384.9	−737.7	−542.0	78.8	−395.7	−71.0	−70.2	−141.2	−781.2	1.17				
Vio7	−1377.5	−725.4	−546.1	74.7	−398.7	−65.3	−60.2	−125.5	−780.5	1.77				
Vio8	−1371.8	−719.7	−543.6	77.2	−398.4	−61.5	−60.4	−121.9	−782.0	1.20				
Vio9	−1405.5	−717.6	−539.0	81.8	−395.6	−64.4	−60.2	−124.6	−824.5	1.68				
Vio10	−1416.5	−712.4	−529.5	91.3	−390.8	−65.1	−62.6	−127.7	−837.3	1.45				

E_{HDC}, energy of the heptamer–drug complex with counterions; E_{HD}, energy of the heptamer–drug complex without counterions; E_{helix}, energy of the helix part of the complex; E_{destab}, difference in energies of the helix part of the complex and the helix energy refined in the absence of the drug; $E_{c\text{-}5}$ energy of the central five base-paired nucleotides in the heptamer; $E_{H\text{-}D1}$, heptamer–acridine 1 interaction energy; $E_{H\text{-}D2}$, heptamer–acridine 2 interaction energy; $E_{H\text{-}D}$, total intercalator–heptamer interaction energies; $E_{H\text{-}Cl}$, total counterion–heptamer interaction energies; $E_{D1\text{-}D2}$, interaction energy between acridine 1 and acridine 2. The Oby structures correspond to neighbor-exclusion model, and the Vio structures correspond to models in which the neighbor-exclusion principle is violated. The structures Oby1 and Vio1 correspond to molecular mechanics simulations without counterions, while the structures Oby2 (Vio2) to Oby10 (Vio10) correspond to molecular dynamics and molecular mechanics simulations (with counterions). The internal energies of the two acridines in all the calculations are nearly identical and have values of −20.8 kcal/mol on the average. S (in cal·mol^{-1}·K^{-1}) is the entropy of the system as derived from the thermochemistry analysis in the normal mode analysis program. N1, N2, and N3 are the three lowest normal modes in cm^{-1}.

ties, all one should conclude is that the two classes of structures are close in energy.

The normal mode analysis and thermochemistry calculations indicate that the complex in which the neighbor-exclusion principle is obeyed has a higher entropy than the structure where this principle is violated. This difference of 8 cal·mol^{-1}·K^{-1} (see Table 2) corresponds to an energy difference of 2.4 kcal/mol at 300 K. This entropy difference could arise as a result of the stiffening of the helical structure due to double intercalation more in the Vio model than in Oby (see Figs. 2 and 3). The greater rigidity in the Vio1 and Vio1′ models compared to Oby1 is reflected in the fact that their low-frequency modes are higher (Table 2). Thus, it is interesting to note that drug–helix entropy considerations qualitatively favor the structures in which the neighbor-exclusion principle is obeyed.

DISCUSSION

We have attempted to focus on the energetic and thermochemical basis for the lack of intercalation models in which the neighbor-exclusion principle is violated. Molecular mechanical and dynamical simulations have been carried out on intercalation models in which the neighbor-exclusion principle is obeyed and on models in which it is violated. We find that it is possible to build stereochemically favorable models in the two classes of structures that are comparable in energy. In the literature, the nearest-neighbor exclusion has been associated with certain combinations of the conformational parameters in the nucleotides involved in intercalative binding. Sobell *et al.* (6), using the crystal-structure analysis of intercalation complexes with dinucleoside monophosphates as a basis, postulated that a mixed sugar puckering scheme C3′ *endo*-3′,5′-C2′ *endo* was necessary in all intercalative binding, thus rationalizing the neighbor-exclusion principle. Subsequently, however, sugar pucker was recognized to be not the only factor in the creation of intercalation sites. In fact, model-building studies on intercalators in A-DNA and A-RNA suggested that during intercalation, all the sugars could retain the characteristic C3′ *endo* pucker. Base open states could be created by variation of the torsions about P—O3′ and C5′—C4′. Later crystal studies have shown that in addition to sugar geometry, the glycosidic torsion and the O5′—C5′ rotation are important conformational determinants in creating intercalation sites. Our studies emphasize the role of nucleic acids backbone flexibility in creating both neighbor-exclusion and non-neighbor-exclusion sites.

Earlier studies on model systems, representing structures in which the neighbor-exclusion principle is violated and obeyed, could not address the stereochemical issue because they merely calculated base-stacking energies (21). In addition, these studies found the difference between the two classes of models to be ≈68 kcal/mol, and on this basis it was concluded that nearest-neighbor intercalation models could be formed as easily as the neighbor-exclusion models. We have, on the other hand, considered a long enough oligonucleotide chain to create the intercalation sites in realistic DNA models.

Miller and Pycior (20) have reported model-building studies on tetranucleotides in the B form (without the explicit presence of the intercalating ligand) with a view to rationalize the geometrical parameters associated with neighbor-exclusion-obeying and -violating intercalation sites by considering variations in backbone and glycosidic torsions. Unlike our energy minimization investigations in which all the degrees of freedom have been varied, that study was done with the constraints of obtaining helical structures that could be embedded in an idealized B-DNA helix. Under these constraints, they found that all the sugars in the intercalation sites had C3′ *endo* pucker, consistent with model-building studies on A form of polynucleotides. In contrast, our neighbor-exclusion-violation models have predominantly C2′ *endo* pucker. Further, in ref. 20 the other five backbone

angles in a mononucleotide were either *trans* or intermediate between *trans* and *gauche*$^-$, and the glycosidic torsions were higher by 20° to 30° than in our models. Based on the conformational features they suggested (20) a low possibility of occurrence of neighbor-exclusion-violating models in short oligonucleotide chains but did not exclude the possibility in a polymer.

Polyelectrolyte effects have been shown to be important in the anticooperativity effects in the cases of ethidium and actinomycin binding to DNA (17). Upon the inclusion of such effects, it was shown unnecessary to invoke multiple-site exclusion to explain the binding. Thus, counterion effects could be important in competition between the two classes of models under study. The entropic and enthalpic contributions obtainable from the release of counterions into the solution, as a result of intercalation of positively charged acridines, could favor the neighbor-exclusion model. In the Vio model, the counterion release would be less because the presence of another intercalator at ≈7 Å has already "released" some of the cations in the vicinity. In the molecular dynamically simulated models, we do see a more favored interaction-energy profile between the heptamer and counterions in Oby than in Vio models. To further assess the counterion effects in complexes involving charged intercalators, similar studies with neutral species such as actinomycin D are in order. In view of the charged nature of our system and the simple treatment of electrostatic effects in our force field, it is clear that electrostatic interactions have not been quantitatively simulated here. Unfortunately, "simple" neutral intercalators do not interact very well with DNA.

CONCLUSIONS

In summary, we could consider four contributions to the relative free energies of neighbor-exclusion-violating and neighbor-exclusion-obeying double-intercalation complexes between DNA and simple intercalators like acridine. The four are stereochemical energies, vibrational entropy, counterion release, and specific solvent–solute interactions. Our results suggest that stereochemical energies cannot be used to rule out the neighbor-exclusion-violating structures. The two classes of models are energetically similar within the limits of accuracy in our force field and simple model. On the other hand, our results suggest that vibrational entropy considerations could play an important role in favoring the more flexible neighbor-exclusion structure over the more rigid neighbor-exclusion-violating structure. Even though the energy difference associated with this entropy difference is smaller than the internal energy difference (Table 2), it is expected to be far less sensitive to an accurate representation of solvent environment.

One of the referees has pointed out that the effects that prevent nearest-neighbor intercalation could come into play only when the acridines intercalate into long stretches of nucleic acids. However, it may be noted that spectroscopic studies (15, 16) that find no evidence for the violation of the neighbor-exclusion principle involve the intercalation of two acridines connected at N9 positions through a series of linker chains into a pentanucleotide double helix. Thus, it is clear that the neighbor-exclusion rule holds for smaller DNA fragments. Therefore, it is likely that our model of a heptanucleotide should be adequate to understand the physical basis of the neighbor-exclusion principle.

Counterion release could be an important factor in destabilizing the latter class of structures. In the framework of the force field employed, we cannot explicitly consider such counterion release effects; however, insight into the significance of this effect could be obtained by looking at ionic-strength-dependent effects or intercalation by neutral analogs of the simple intercalators. Of course, there has been no explicit inclusion of solvent interactions in these simulations. Thus, we cannot rule out that solute–solvent interactions or differences in solvent–solvent interactions could influence the relative energies of neighbor-exclusion-violating and -obeying structures. More extensive simulations including both counterions and solvent will be required to assess the possible role of counterions and solvent in providing a more precise energetic basis for the neighbor-exclusion rule.

We thank Dr. U. Chandra Singh for his help with the normal mode analysis program in AMBER(UCSF). We gratefully acknowledge the support from Grant CA-25644 from the National Cancer Institute in this research. The use of the facilities of the University of California, San Francisco, Computer Graphics Laboratory (R. Langridge, director, and T. Ferrin, facility manager), supported by Grant RR-1081 from the National Institutes of Health, is also gratefully acknowledged. The purchase of the FPS-264 array processor was made possible through Grants RR-02441 from the National Institutes of Health and DMB-84-13762 from the National Science Foundation, and their support for this is much appreciated.

1. Crothers, D. M. (1968) *Biopolymers* **6**, 575–584.
2. Bond, P. J., Langridge, R., Jennette, K. W. & Lippard, S. J. (1975) *Proc. Natl. Acad. Sci. USA* **72**, 4825–4829.
3. Arnott, S., Bond, P. J. & Chandrasekaran, R. (1980) *Nature (London)* **287**, 561–563.
4. Tsai, C., Jain, S. C. & Sobell, H. M. (1977) *J. Mol. Biol.* **114**, 301–315.
5. Jain, S. C., Tsai, C. & Sobell, H. M. (1977) *J. Mol. Biol.* **114**, 317–331.
6. Sobell, H. M., Tsai, C., Jain, S. C. & Gilbert, S. G. (1977) *J. Mol. Biol.* **114**, 333–365.
7. Neidle, S., Achari, A., Taylor, G. L., Berman, H. M., Carrell, H. L., Glukser, J. P. & Stallings, W. C. (1977) *Nature (London)* **269**, 304–307.
8. Berman, H. M., Stallings, W. C., Carrell, H. L., Glukser, J. P., Neidle, S., Taylor, G. L. & Achari, A. (1979) *Biopolymers* **18**, 2405–2429.
9. Nelson, J. W. & Tinoco, I., Jr. (1984) *Biopolymers* **23**, 213–233.
10. Alden, C. J. & Arnott, S. (1975) *Nucleic Acids Res.* **2**, 1701–1717.
11. Alden, C. J. & Arnott, S. (1977) *Nucleic Acids Res.* **4**, 3855–3861.
12. Wakelin, L. P. G., Romanos, M., Chen, T. K., Glaubiger, D., Canellakis, E. S. & Waring, M. J. (1978) *Biochemistry* **17**, 5057–5063.
13. Atwell, G. J., Leupin, W., Twigden, S. J. & Denny, W. A. (1983) *J. Am. Chem. Soc.* **105**, 2913–2914.
14. Denny, W. A., Atwell, G. J., Baguley, B. C. & Wakelin, L. P. G. (1985) *J. Med. Chem.* **28**, 1568–1574.
15. Assa-Munt, U., Denny, W. A., Leupin, W. & Kearns, D. R. (1985) *Biochemistry* **24**, 1441–1449.
16. Assa-Munt, U., Leupin, W., Denny, W. A. & Kearns, D. R. (1985) *Biochemistry* **24**, 1449–1460.
17. Friedman, R. A. G. & Manning, G. S. (1984) *Biopolymers* **23**, 2671–2714.
18. Quigley, G. J., Wang, A. H.-J., Ughetto, G., van der Marel, G., van Boom, J. H. & Rich, A. (1980) *Proc. Natl. Acad. Sci. USA* **77**, 7204–7208.
19. Wang, A. H.-J., Ughetto, G., Quigley, G. J., Hakoshima, T., van der Marel, G. A., van Boom, J. H. & Rich, A. (1984) *Science* **225**, 1115–1121.
20. Miller, K. J. & Pycior, J. F. (1979) *Biopolymers* **18**, 2683–2719.
21. Sawaryn, A., Leps, B. & Bradaczek, H. (1983) *J. Comp. Chem.* **4**, 333–336.
22. Dearing, A. (1981) CHEM, A Molecular Display Program (Univ. of California, San Francisco).
23. Weiner, P. K. & Kollman, P. A. (1981) *J. Comp. Chem.* **2**, 287–310.
24. Weiner, P. K., Singh, U. C., Kollman, P. A., Caldwell, J. W. & Case, D. (1985) AMBER, A Molecular Mechanics and Dynamics Program (Univ. of California, San Francisco), Version 2.0.
25. Singh, U. C., Weiner, P. K., Caldwell, J. W. & Kollman, P. A. (1986) AMBER, A Molecular Mechanics and Dynamics Program (Univ. of California, San Francisco), Version 3.0 (developed for FPS).
26. Weiner, S. J., Kollman, P. A., Case, D., Singh, U. C., Ghio, C., Alagona, J., Profeta, S., Jr., & Weiner, P. K. (1984) *J. Am. Chem. Soc.* **106**, 765–785.
27. Singh, U. C. & Kollman, P. A. (1984) *J. Comp. Chem.* **5**, 129–144.
28. Singh, U. C., Weiner, S. J. & Kollman, P. A. (1985) *Proc. Natl. Acad. Sci. USA* **82**, 755–759.
29. Arnott, S., Campbell-Smith, P. & Chandrasekaran, R. (1976) in *CRC Handbook of Biochemistry*, ed. Fasman, G. D. (CRC, Cleveland, OH), Vol. 2, pp. 411–422.
30. Seeman, N. C., Rosenberg, J. M., Suddath, F. L., Kim, J. J. P. & Rich, A. (1976) *J. Mol. Biol.* **104**, 109–144.
31. Sakore, T. D., Reddy, B. S. & Sobell, H. M. (1979) *J. Mol. Biol.* **135**, 763–785.
32. Kim, S. H. (1981) in *Topics in Nucleic Acid Structure*, ed. Neidle, S. (Wiley, New York), pp. 83–112.
33. Yathindra, N. & Sundaralingam (1975) *Biopolymers* **14**, 2387–2404.
34. Saenger, W. (1984) *Principles of Nucleic Acid Structure* (Springer, New York), pp. 51–101.
35. Wang, J. C. (1974) *J. Mol. Biol.* **89**, 783–801.